Disordering and Mixed Conductivity in the Solid Solution $LaSr_2Fe_{3-y}Cr_yO_{8+\delta}$

Victor L. Kozhevnikov,*,† Ilia A. Leonidov,† Julia A. Bahteeva,† Mikhail V. Patrakeev,† Edward B. Mitberg,† and Kenneth R. Poeppelmeier‡

Institute of Solid State Chemistry, Ural Branch of Russian Academy of Sciences, 91 Pervomaiskaia, GSP-145, Ekaterinburg 620219, Russia, and Department of Chemistry, Northwestern University, 2145 Sheridan Road, Evanston Illinois, 60208

Received May 19, 2003. Revised Manuscript Received April 26, 2004

Ceramic samples of $LaSr_2Fe_{3-y}Cr_yO_{8+\delta}$ ($y = 0$, 0.3, 0.6, and 1.0) were characterized with X-ray powder diffraction, thermal gravimetry, dilatometry, and total conductivity measurements in the temperature range 750−950 °C at oxygen partial pressures between 10^{-22} and 0.5 atm. When prepared in air, the doped ferrites adopt rhombohedral $R\bar{3}c$ structure. The loss of oxygen from the crystal lattice results in formation of the vacancy-ordered orthorhombic structure $LaSr_2Fe_3O_8$ for the parent ferrite at temperatures above 750 °C and oxygen pressures below about 10^{-5} atm while chromium substituted samples retain the rhombohedral structure. The isothermal ion conductivity is found to decrease with the increase in chromium doping from $y = 0$ to $y = 0.6$. However, an increase in the chromium content to $y = 1$ results in an increase in the oxygen ion conductivity to about 0.2 S/cm. This behavior is explained with a model where the oxygen ions coordinated to chromium are not excluded entirely from the transport mechanism.

Introduction

Various changes such as aliovalent doping, temperature, and the oxygen pressure in the ambient atmosphere result in the formation of oxygen vacancies in the crystalline lattice of oxide perovskites. When present in sufficient amount, oxygen vacancies can form long-range ordered structures.[1−8] These ordered vacancies can become unavailable for diffusion of oxygen ions and are, therefore, considered as unfavorable for ion migration. In contrast to this general consideration, significant oxygen ion conductivity, which follows from the high oxygen permeation fluxes reported, was reported by Schwartz et al.[9] in the solid solution $La_{1-x}Sr_xFe_{1-y}Ga_yO_{3-\delta}$ ($x = 0.1-0.4$; $y = 0.2-0.5$) which adopts an oxygen vacancy ordered brownmillerite structure. The large ion conductivity (~0.2 S/cm at 950 °C) in the similar, brownmillerite-like oxide $Sr_2Fe_2O_5$ is explained as caused by a partial, temperature-driven disordering of the structural vacancies.[10] The disorder is not sufficient, however, to result in the transformation of the brownmillerite structure to that of the perovskite.

Another vacancy ordered ferrite $LaSr_2Fe_3O_8$ was described by Battle et al.[11] It can be envisioned as derived from the perovskite structure where regular arrangement of oxygen vacancies results in tripling of the elementary unit with double layers of iron−oxygen octahedra (FeO_3) that alternate with the single layers of iron−oxygen tetrahedra (FeO_2). The oxygen ion conductivity in $LaSr_2Fe_3O_8$ achieves about 0.35 S/cm at 950 °C,[12] which is larger than in the brownmillerite-like $Sr_2Fe_2O_5$ while it is smaller than in the perovskite-like $La_{0.5}Sr_{0.5}FeO_{2.75}$ (~0.45 S/cm at 950 °C).[13] Considering that the amount of oxygen vacancies is larger in $LaSr_2Fe_3O_8$ ($La_{0.33}Sr_{0.67}FeO_{2.67}$) than in $La_{0.5}Sr_{0.5}FeO_{2.75}$ the conclusion can be made that heating to rather high temperatures cannot overwhelm completely partial ordering of the oxygen vacancies in $LaSr_2Fe_3O_8$. Partial doping of iron sub-lattice may help to additionally disorder the structural vacancies and, thus, to increase the ion conductivity level.

In this study we report on the solid solution $LaSr_2Fe_{3-y}Cr_yO_8$. The electrical conductivity measurements are carried out in the temperature interval 750−950 °C

* To whom correspondence should be addressed. Tel: +7 (3432) 78 36 61. Fax: +7 (3432) 74 00 03. E-mail: kozhevnikov@imp.uran.ru.
† Ural Branch of Russian Academy of Sciences.
‡ Northwestern University.

(1) Rao, C. N. R.; Gopalakrishnan, J.; Vidyasagar, K. *Ind. J. Chem.* **1984**, *23A*, 265.
(2) Takeda, Y.; Kanno, K.; Takada, T.; Yamamoto, O.; Takano, M.; Nakayama, N.; Bando, Y. *J. Solid State Chem.* **1986**, *63*, 237.
(3) Grenier, J.-C.; Ea, N.; Puchard, M.; Hagenmuller, P. *J. Solid State Chem*. **1985**, *58*, 243.
(4) Alario-Franco, M. A.; Henche, M. J. R.; Valet, M.; Calbet, J. M. G.; Grenier, J.-C.; Wattiaux, A.; Hagenmuller, P. *J. Solid State Chem*. **1983**, *46*, 23.
(5) Calbet, J. M. G.; Vallet-Regi, M.; Alario-Franco, M. A.; Grenier, J.-C. *Mater. Res. Bull.* **1983**, *18*, 285.
(6) Fournès, L.; Potin, Y.; Grenier, J.-C.; Demazeau, G.; Pouchard, M. *Solid State Commun*. **1987**, *62*, 239.
(7) Takano, M.; Okita, T.; Nakayama, N.; Bando, Y.; Takeda, Y.; Yamamoto, O.; Goodenough, J. B. *J. Solid State Chem*. **1988**, *73*, 140.
(8) Calbet, J. M. G.; Parras, M.; Vallet-Regi, M.; Grenier, J.-C. *J. Solid State Chem.* **1991**, *92*, 110.
(9) Schwartz, M.; White, J.; Sammels, A. Int. Patent Appl. PCT/US96/14841, WO 97/41060, 1997.
(10) Kozhevnikov, V. L.; Leonidov, I. A.; Patrakeev, M. V.; Mitberg, E. B.; Poeppelmeier, K. R. *J. Solid State Chem*. **2000**, *158*, 320.
(11) Battle, P. D.; Gibb, T. C.; Lightfoot, P. *J. Solid State Chem.* **1990**, *84*, 237.
(12) Leonidov, I. A.; Kozhevnikov, V. L.; Patrakeev, M. V.; Mitberg, E. B.; Poeppelmeier, K. R. *Solid State Ionics* **2001**, *144*, 361.
(13) Patrakeev, M. V.; Bahteeva, J. A.; Mitberg, E. B.; Leonidov, I. A.; Kozhevnikov, V. L.; Poeppelmeier, K. R. *J. Solid State Chem.* **2003**, *172*, 219.

10.1021/cm031084o CCC: $27.50
Published on Web 11/06/2004

and partial oxygen pressure range 10^{-22} to 0.5 atm. The results are used in combination with X-ray powder diffraction and thermogravimetry data to analyze variations in the ion and electron contributions to the total conductivity with oxygen pressure and chromium content. The partial ion contribution and total conductivity data are used to evaluate the oxygen permeation fluxes through 0.1 cm thick ceramic membranes, which, when combined with thermal expansion measurements, demonstrate their potential for the partial oxidation of methane to syngas.

Experimental Section

The samples of $LaSr_2Fe_{3-y}Cr_yO_{8+\delta}$ used in this study were prepared by solid-state reactions. Starting materials were the oxides Fe_2O_3 (99.2%), Cr_2O_3 (99.4%), La_2O_3 (99.96%), and strontium carbonate $SrCO_3$ (99.94%). The raw materials were precalcined to remove adsorbates. Appropriate amounts were weighed and thoroughly mixed with a mortar and pestle with the addition of ethanol. The mixtures were pressed into pellets and fired several times from 750 to 1300 °C in air. The materials were crushed into powder, pressed, and fired with a gradual increase in temperature before single-phase specimens were obtained. Phase purity and determination of the lattice parameters were carried out with the help of X-ray diffraction using a STADI-P (STOE) diffractometer in Bragg−Brentano geometry (Cu Kα radiation; 2Θ range of 5−120°; step 0.02°). For better statistics the acquisition time at every angle was 20 s. The reduction experiments and studies of oxygen content changes in the specimens as a function of temperature were carried out with a Setaram TG-DTA-92 thermoanalyzer in the gas mixture 90:10 He/H_2. The reduction process was carried out until the oxide composition $LaSr_2Fe_{3-y}Cr_yO_8$ was achieved with iron and chromium cations in +3 oxidation state. Then, the respective weight loss was used to calculate the oxygen content in the initial sample $LaSr_2Fe_{3-y}Cr_yO_{8+\delta}$.

The synthesized materials were again ball-milled in ethanol and pressed into disks under 2 kBar uniaxial load. The disks were sintered in air at 1300−1350 °C for 10 h to a density no less than 90% of theoretical. Part of the ceramic samples were shaped in the form of parallelepipeds 4 × 4 × 8 mm for measurements of thermal expansion with the help of a DL-1500RHP dilatometer (Ulvac Sinku-Riko); the heating rate was 3°/min. Also, rectangular bars 2 × 2 × 15 mm were cut from the sintered disks for the four-probe dc conductivity measurements. Potential probes and current leads were made of 0.3 mm Pt wire and tightly wound to the specimen with 7 and 12 mm spacing, respectively. It is important to note that platinum metal is known as a reversible oxygen electrode. Therefore, the use of platinum probes and leads ensures that the conductivity measurements reflect the oxygen ion contribution together with the electronic, n- and p-type, contribution. The wired specimen was sealed under an atmosphere containing 50% O_2 and 50% CO_2 in the measuring cell of stabilized cubic zirconia. The cell was equipped with two pairs of Pt electrodes. One pair was used as oxygen pump to change and maintain oxygen partial pressure (pO_2) while the other was utilized as oxygen sensor in order to independently control the pO_2 inside the cell. The assembly was set in the isothermal zone of a tubular furnace where the temperature was maintained accurately. The electrical parameters were measured with a high-precision Solartron 7081 voltmeter. Computer-controlled operation of the oxygen pump and sensor provided precise variation and maintenance of the oxygen partial pressure in the cell. The measurements were carried out in the mode of decreasing oxygen partial pressure in isothermal runs. The relaxation time after a change in the oxygen pressure over a sample varied and was dependent on the temperature and oxygen partial pressure range. The accepted criterion for having achieved equilibrium was a relaxation rate change of less than 0.1% per minute in the logarithm of the conductivity while at a fixed oxygen pressure inside the cell.

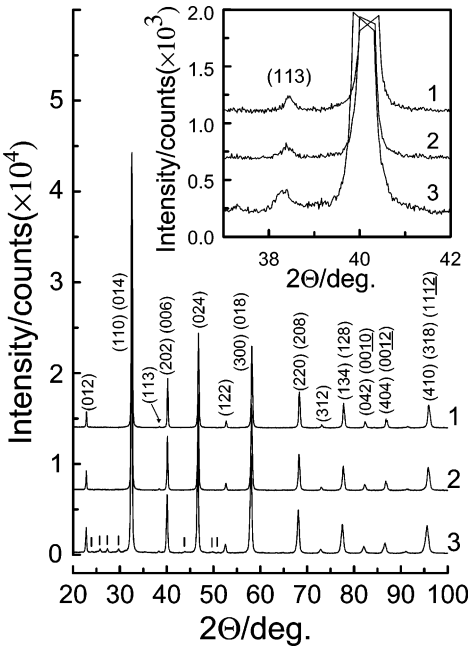

Figure 1. X-ray powder diffraction patterns for the air-prepared samples $LaSr_2Fe_{3-y}Cr_yO_{8+\delta}$ at different chromium content $y = 0.3$ (1), 0.6 (2), 1.0 (3). Strokes on pattern (3) point to peaks of $SrCrO_4$. The 2Θ area at 37−42 degrees is shown enlarged in the inset.

Table 1. Elementary Unit Parameters for $LaSr_2Fe_{3-y}Cr_yO_{8+\delta}$ Equilibrated in Different Atmospheres

atmosphere	y	a, Å	c, Å	V, Å^3
air	0.3	5.4894(2)	13.4156(6)	350.57
	0.6	5.4939(1)	13.4189(5)	350.78
	1.0	5.5094(5)	13.4476(8)	353.76
10:90 H_2/He	0.3	5.5272(1)	13.5310(3)	357.97
	0.6	5.5217(2)	13.5182(1)	356.94
	1.0	5.5202(4)	13.5082(6)	356.48

Results and Discussion

1. Sample Characterization. Samples of $LaSr_2Fe_{3-y}Cr_yO_{8+\delta}$, where $y = 0$, 0.3, 0.6, and 1, were equilibrated at 1200−1300 °C and slowly cooled in the air. On the basis of their powder X-ray diffraction patterns, Figure 1, it was evident that all specimens adopt a perovskite-like structure similar to that of $LaSr_2Fe_3O_{8+\delta}$.[14] The compositions with $0 \le y \le 0.6$ were single-phase oxides, while a small amount of the $SrCrO_4$ admixture phase was observed in the sample with $y = 1$. During the course of the analysis of the obtained X-ray data it became clear that the peaks at higher angles were somewhat broadened thus indicating several poorly resolved reflections. Therefore, the attempt was made to index the X-ray spectra with the $R\bar{3}c$ space group. The indexing was confirmed by observation of the small peak (113) near 2Θ = 38°, Figure 1 (inset). The diffraction lines shift to lower angles thus showing an increase of the elementary unit parameters with chromium content, Table 1. When heated in the flow of 10:90 H_2/He gas mixture, the air-synthesized samples of $LaSr_2Fe_{3-y}Cr_yO_{8+\delta}$ exhibit considerable loss of weight corresponding to oxygen homogeneous region δ ranging from about −0.2 to 1, Figure 2. The oxygen stoichiometry in the air-prepared samples was found to cor-

(14) Battle, P. D.; Gibb, T. C.; Lightfoot, P. *J. Solid State Chem.* **1990**, *84*, 271.

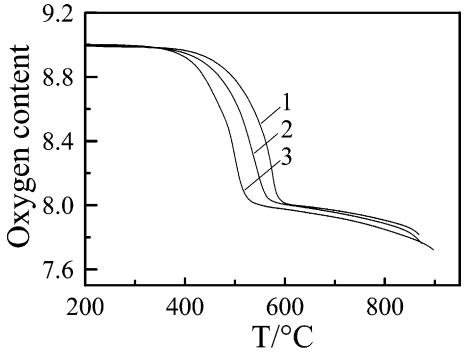

Figure 2. Oxygen content changes in the air-synthesized samples $LaSr_2Fe_{3-y}Cr_yO_{8+\delta}$, $y = 0.3$ (1), 0.6 (2), 1.0 (3), at heating in 10:90 H_2/He gas mixture.

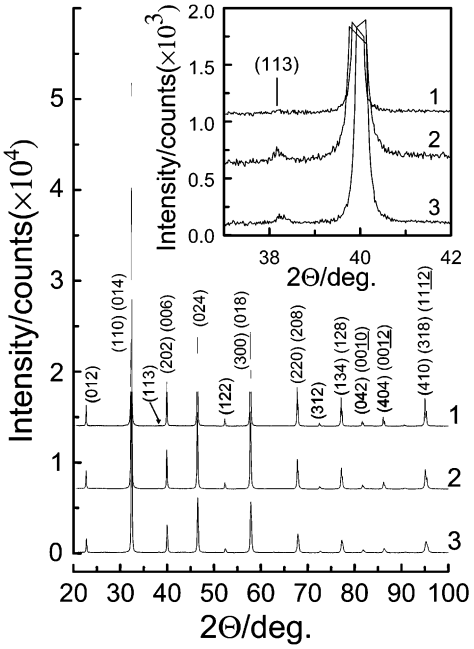

Figure 3. X-ray powder diffraction patterns for $LaSr_2Fe_{3-y}Cr_yO_8$ at different chromium content $y = 0.3$ (1), 0.6 (2), 1.0 (3). The 2Θ area at 37−42 degrees is shown enlarged in the inset.

respond to $\delta = 1$, i.e., to the formula $LaSr_2Fe_{3-y}Cr_yO_9$, regardless of the doping level.

The removal of one oxygen atom from $LaSr_2Fe_3O_9$ results in the vacancy ordered orthorhombic perovskite-like structure of $LaSr_2Fe_3O_8$.[11] At the same time, the heating of the chromium doped specimens to 570−590 °C in the 10:90 H_2/He gas mixture results in formation of $LaSr_2Fe_{3-y}Cr_yO_8$ samples having X-ray spectra similar to those of the initial $LaSr_2Fe_{3-y}Cr_yO_9$, Figure 3. It may be added here that such a heat treatment resulted in disappearance of the trace admixture $SrCrO_4$ from the sample with $y = 1$. Again, some broadening of the lines at higher angles and observation of the very weak reflection near $2\Theta = 38°$, Figure 3 (inset), suggested indexing of the X-ray spectra for $LaSr_2Fe_{3-y}Cr_yO_8$ with the $R\bar{3}c$ space group.

The concentration-dependent behavior of the rhombohedral angle a_{rhomb} is indicative of the rhombohedral distortions increasing with chromium content in both $LaSr_2Fe_{3-y}Cr_yO_9$ and $LaSr_2Fe_{3-y}Cr_yO_8$, Figure 4. It can be seen from Figure 4 that the increase in the amount of chromium in $LaSr_2Fe_{3-y}Cr_yO_8$ is accompanied

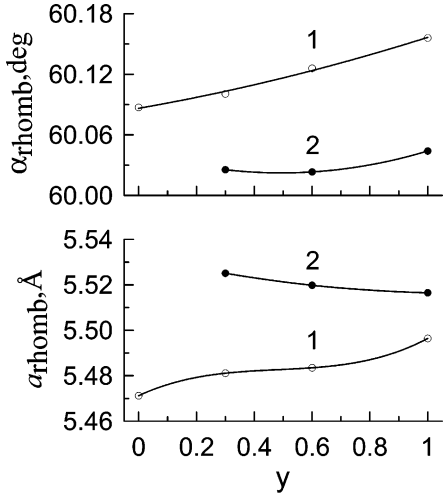

Figure 4. Variations in the elementary unit parameters with chromium content in $LaSr_2Fe_{3-y}Cr_yO_9$ (1) and $LaSr_2Fe_{3-y}Cr_yO_8$ (2).

with the decrease of the rhombohedral elementary unit parameter a_{rhomb}. Such a change reflects replacement of the larger Fe^{3+} for smaller Cr^{3+} cations ($r_{VI}(Fe^{3+}) = 0.645$ Å; $r_{VI}(Cr^{3+}) = 0.615$ Å[15]). This conclusion is corroborated by comparison of the formula unit volumes for $LaFeO_3$ and $LaCrO_3$ perovskites that are equal to 60.72 and 58.63 Å^3, respectively.[16,17] In contrast, the lattice parameter a_{rhomb} in the oxidized phase $LaSr_2Fe_{3-y}Cr_yO_9$ tends to increase with chromium content, which seems surprising. Indeed, Cr^{4+} cations are no less stable than Fe^{4+} cations in perovskite-like oxides as follows from comparison of thermodynamic properties of $La_{1-x}Sr_xCrO_3$ and $La_{1-x}Sr_xFeO_3$ at elevated values of temperature and oxygen partial pressure.[18,19] Hence, chromium substitution for iron in the parent oxide $LaSr_2Fe^{3+}Fe_2^{4+}O_9$, where iron is in the mixed 3+/4+ oxidation state,[14] proceeds as replacement of Fe^{4+} for Cr^{4+} cations with formation of $LaSr_2Fe^{3+}Fe_{2-y}^{4+}Cr_y^{4+}O_9$. Therefore, one can expect some contraction of the crystal lattice and a decrease in a_{rhomb} because of the cation size difference ($r_{VI}(Fe^{4+}) = 0.585$ and $r_{VI}(Cr^{4+}) = 0.55$ Å[15]). The observed increase in the lattice parameter can be attributed to 3d metal−2p oxygen covalent overlap smaller for $Cr^{4+}-O^{2-}$ than for $Fe^{4+}-O^{2-}$ chemical bonds. The smaller covalence results in decrease of the bonding energy and in respective increase of the average length of metal−oxygen bonds, which overwhelms the cation size effect and gives rise to an increase in the lattice parameter $a_{r\ hom\ b}$. This conclusion is consistent with the shift of the oxygen depletion process to smaller temperatures at heating of $LaSr_2Fe_{3-y}Cr_yO_9$ with larger amount of chromium, Figure 2.

The transformation of the orthorhombic structure of $LaSr_2Fe_3O_8$ into the rhombohedral structure of the solid solution $LaSr_2Fe_{3-y}Cr_yO_8$ can be understood assuming

(15) Shannon, R. D. *Acta Crystallogr. A.* **1976**, *32*, 751.
(16) Dann, S. E.; Currie, D. B.; Weller, M. T.; Thomas, M. F.; Al-Rawwas, A. D. *J. Solid State Chem.* **1994**, *109*, 134.
(17) International Centre for Diffraction Data. Database JCPDS, 33-0701.
(18) Mizusaki, J.; Yamauchi, S.; Fueki, K.; Ishikawa, A. *Solid State Ionics* **184**, *12*, 119.
(19) Mizusaki, J.; Yoshihiro, M.; Yamauchi, S.; Fueki, K. *J. Solid State Chem.* **185**, *58*, 257.

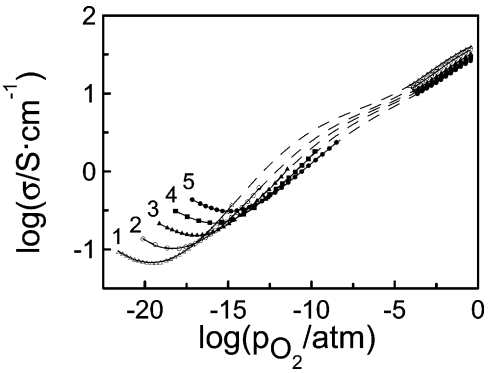

Figure 5. Logarithmic plots of the total conductivity versus oxygen pressure for the oxide $LaSr_2Fe_{3-y}Cr_yO_{8+\delta}$ at different temperatures: (1) 750, (2) 800, (3) 850, (4) 900, (5) 950 °C; lines serve as guides for the eye.

a statistical distribution of the dopant. That is, approximately two-thirds of the chromium cations replace iron in octahedral sites while the remaining one-third substitute for iron in tetrahedral sites. When chromium replaces iron on a tetrahedral site, a number of events occur in the crystal lattice. First, this tetrahedron transforms to an octahedron because of the preference of chromium to maintain 6-fold coordination. The corresponding amount of oxygen, which is necessary to form the octahedral environment around chromium, is scavenged from the octahedral surrounding of iron cations, thus transforming respective octahedral (FeO_3) to pyramids ($FeO_{2.5}$). Simultaneously, two other (FeO_2) tetrahedra, which are neighbors to the newly formed octahedron (CrO_3), also become pyramids ($FeO_{2.5}$). Thus, the replacement of *one* iron cation on a tetrahedron site by chromium results in the change of *five* structural polyhedra. Consequently, the crystal-chemical formula of the solid solution can be presented as $LaSr_2(FeO_3)_{2-2y}(CrO_3)_y(FeO_{2.5})_{2y}(FeO_2)_{1-y}$, and, according to the formula, the amount of iron−oxygen tetrahedra in $LaSr_2Fe_{3-y}Cr_yO_8$ progressively decreases with the increase in chromium content. Owing to the random distribution of chromium, the tetrahedra also disappear in a random fashion. This, in turn, results in randomization of the initial order of octahedral and tetrahedral layers and the rapid transformation of the parent orthorhombic structure of $LaSr_2Fe_3O_8$ into the nearly cubic structure of $LaSr_2Fe_{3-y}Cr_yO_8$ with small rhombohedral distortions.

2. Analysis of Total Conductivity. Logarithmic plots of the equilibrium total conductivity versus the partial pressure of oxygen at different temperatures are shown in Figure 5 for the oxide with $y = 1$ as an example. The regions between the low- and high-pressure extremes are shown with dashed lines because of the slow equilibration kinetics in the middle-pressure range, which make obtaining reliable equilibrium data a very lengthy and difficult process.[13] Only the low-pressure segments of the isotherms lg $\sigma \div$ lg pO_2 near the minima, where deviations of the oxygen content from the nominal stoichiometric composition are very small, i.e., $\delta \ll 1$, are important for the analysis of the oxide ion contribution. Such minima are typical in oxides when oxygen pressure variations at constant temperature result in nearly equal concentrations of electron- and hole-like carriers. There may be another, pressure independent contribution in the conductivity

Table 2. Conductivity Parameters in $LaSr_2Fe_{3-y}Cr_yO_8$ as Obtained by Fitting Eq 1 to Experimental Data[a]

		temperature, °C				
y	parameter	950	900	850	800	750
0	σ_i°	0.34	0.26	0.19	0.14	0.09
	σ_n°	$13.2\cdot10^{-5}$	$5.4\cdot10^{-5}$	$2.0\cdot10^{-5}$	$6\cdot10^{-6}$	$2\cdot10^{-6}$
	σ_p°	75	96	123	151	181
0.3	σ_i°	0.14	0.11	0.07	0.05	0.03
	σ_n°	$4.0\cdot10^{-5}$	$1.6\cdot10^{-5}$	$6\cdot10^{-6}$	$2\cdot10^{-6}$	$6\cdot10^{-7}$
	σ_p°	60	77	98	130	170
0.6	σ_i°	0.09	0.07	0.05	0.03	0.02
	σ_n°	$2.1\cdot10^{-5}$	$8\cdot10^{-6}$	$3\cdot10^{-6}$	$1\cdot10^{-6}$	$3\cdot10^{-7}$
	σ_p°	100	124	158	216	287
1.0	σ_i°	0.17	0.12	0.08	0.05	0.03
	σ_n°	$1.3\cdot10^{-5}$	$5\cdot10^{-6}$	$2\cdot10^{-6}$	$8\cdot10^{-7}$	$2\cdot10^{-7}$
	σ_p°	357	485	693	944	1430

[a] σ_i° in [S·cm^{-1}], σ_n° in [S·atm$^{1/4}$·cm^{-1}], σ_p° in [S·atm$^{-1/4}$·cm^{-1}].

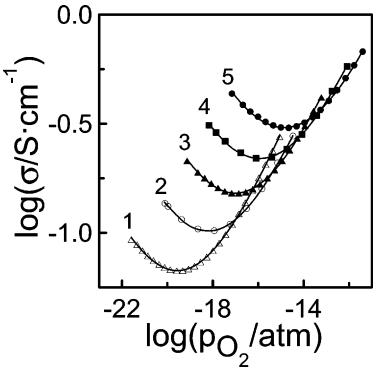

Figure 6. Comparison of the measured conductivity with the results of the conductivity fitting (solid lines) according to eq 1 for the oxide $LaSr_2Fe_{3-y}Cr_yO_{8+\delta}$ ($\delta \ll 1$) at different temperatures: (1) 750, (2) 800, (3) 850, (4) 900, (5) 950 °C.

and its presence is signaled by a smooth shape of the minima. Such a contribution usually is due to ionic current, and when it is significant the minima degenerate into broad intervals of pressure independent conductivity as it occurs in ionic unipolar conductors. With these arguments in mind, the experimental results near the conductivity minima were approximated with the known relation[20]

$$\sigma = \sigma_i + \sigma_n^\circ \cdot pO_2^{-1/4} + \sigma_p^\circ \cdot pO_2^{+1/4} \qquad (1)$$

where σ_i stands for the ion-oxygen contribution while parameters σ_n° and σ_p° denote electron σ_n and hole σ_p contributions to the total conductivity, respectively, as extrapolated to $pO_2 = 1$ atm. The fitting parameters that enable a satisfactory approximation of the experimental data are given in Table 2. A reasonable correspondence of the experimental data and calculations at different temperatures is demonstrated in Figure 6 where comparison is given for the composition with $y = 1$ as an example. The data in Table 2 summarize the temperature and pressure variations of the ion, electron, and hole contributions within pressure limits used in the fitting. For instance, this range extends from 10^{-22} to 10^{-12} atm in Figure 6. It is important to remember that the respective data must be referred to $LaSr_2Fe_{3-y}Cr_yO_{8+\delta}$, $\delta \ll 1$. Caution must be taken with extrapolations to larger oxygen pressures because intensive

(20) Schmalzried, H. *Solid State Reactions*, 2nd ed.; Verlag Chemie: Weinheim, 1981.

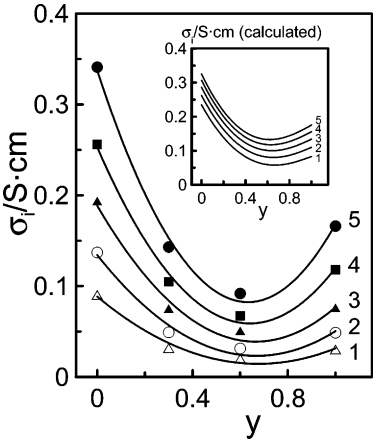

Figure 7. Oxygen ion conductivity dependence versus chromium content in the oxide $LaSr_2Fe_{3-y}Cr_yO_{8+\delta}$ ($\delta \ll 1$) at different temperatures: (1) 750, (2) 800, (3) 850, (4) 900, (5) 950 °C; lines serve as guides for the eye. The inset shows the results of the model calculations.

filling of the oxygen vacancies assists transformation at about 10^{-5} to 10^{-4} atm of the semiconductor $LaSr_2Fe_{3-y}Cr_yO_{8+\delta}$ ($\delta \ll 1$) to the metal-like perovskite $LaSr_2Fe_{3-y}Cr_yO_{8+\delta}$ ($\delta \rightarrow 1$) where dependence of the hole contribution σ_p from oxygen pressure is less strong than the proportionality $\sigma_p \sim pO_2^{+1/4}$. Because the ion conductivity level does not exceed σ_{min} it is believed that the data in the high-pressure limit in Figure 5, where total conductivity achieves 100−200 S/cm, represent with good precision p-type conductivity.

3. Oxygen-Ion Contribution. The doping dependent behavior of the ion conductivity at different temperatures is shown in Figure 7 as obtained from the experimental data using relation 1. Following reference 10, we suggest that the ion transport in $LaSr_2Fe_{3-y}Cr_yO_{8+\delta}$ ($\delta \ll 1$) involves mainly oxygen ions and vacancies in the network of iron−oxygen octahedra and pyramids, while the oxygen ions coordinated by chromium and the oxygen structural vacancies in the first coordination sphere of the tetrahedrally coordinated iron do not take part in the transport. Quite similar to the consideration of the doping induced disorder, we now consider the important role the temperature driven disorder of oxygen (when displacement of an oxygen ion from an FeO_3 octahedron to the structural vacancy near an FeO_2 tetrahedron results in formation of two $FeO_{2.5}$ pyramids) can have with respect to oxygen-ion conductivity. Denoting the equilibrium amount per formula unit of the redistributed oxygen as α, the solid solution may be represented as $LaSr_2(FeO_3)_{2-2y-\alpha}(CrO_3)_y(FeO_{2.5})_{2y+2\alpha}(FeO_2)_{1-y-\alpha}$ where the influence of both temperature and dopant on the relative fractions of structural polyhedra can be seen. Assuming the effective mass law, the equilibrium amounts of the oxygen ions and vacancies in iron−oxygen polyhedra are interrelated as

$$\frac{(2y + 2\alpha)^2}{(2 - 2y - \alpha)(1 - y - \alpha)} = K(T) \qquad (2)$$

The equilibrium constant is given by the ordinary temperature dependence $K(T) = K^\circ \exp(-\Delta H/kT)$, where K° is a constant, ΔH is the disordering enthalpy, and k is the Boltzmann constant. The parameter α follows from eq 2 as a function of the doping level and temperature. Then it can be used to determine the isothermal dependence of the ion conductivity from the doping according to

$$\sigma_i \approx (2 - 2y - \alpha)(2y + 2\alpha) \qquad (3)$$

The first multiplier shows the amount of iron−oxygen octahedra, which, as supposed, is proportional to the amount of the oxygen ions taking part in the transport, while the second one corresponds to the amount of the iron−oxygen pyramids, i.e., oxygen vacancies available for the jumps of the oxygen ions. The model calculations involving relations 2 and 3 result in the monotonic decrease of the ion conductivity within the doping level utilized in this study. This behavior disagrees with the results in Figure 7 where the conductivity increase is seen with the doping increase from $y = 0.6$ to $y = 1$. We suppose, therefore, that the initial assumption that the chromium coordinated oxygen ions are excluded entirely from the transport is too rigid, at least at the doping levels used, and some fraction of these oxygen ions can take part in the transport. For instance, if one CrO_3 octahedron has one corner oxygen shared with another FeO_3 octahedron, the initial supposition would mean exclusion of this oxygen ion from the transport. In the case of two FeO_3 octahedra linked with a CrO_3 octahedron, two respective oxygen ions would be excluded, and so on. The assumption that these "common" oxygen ions may be involved in the transport means that the coefficient before y in the multiplier $(2 - 2y - \alpha)$, see relation 3, must decrease with y and be somewhat smaller than 2. The simplest supposition $(2 - f(y)\cdot y - \alpha)$, where $f(y) = 2 - y$, leads to results which are in semiquantitative agreement with the experiment at reasonable values $K^\circ \approx 1-10$ and $\Delta H \approx 0.2-0.4$ eV, see the inset in Figure 7. Thus, the partial involvement in the ion transport of oxygen ions around chromium sites may help to understand the somewhat larger ion conductivity values for $y = 1$ compared to those for $y = 0.6$. Certainly, this explanation is applicable only to relatively small concentrations of the dopant and when chromium−oxygen octahedra are rather isolated from each other. It is interesting to notice also that similar concentration dependent behavior of the ion conductivity is observed at moderate gallium doping (see Table 2 in ref 21).

4. Electron Conductivity. Pressure dependencies of the sum $\sigma_{n+p} = \sigma_n + \sigma_p$ of electron σ_n and hole σ_p contributions at respective temperatures are obtained by subtraction of the ion conductivity from the isotherms of the total conductivity. The example for $LaSr_2Fe_{3-y}Cr_yO_{8+\delta}$ with $y = 1$ is shown in Figure 8. The isotherms in Figure 8 resemble those in Figure 5, though the minima corresponding to the near equality of σ_n and σ_p are delineated in a sharper manner and each isotherm is shifted downward along the conductivity axis according to the subtracted value of the ion conductivity. The pressure increase/decrease to the right/left of the minima results in prevalence of p/n carriers, which reflects incorporation/release of a small

(21) Leonidov, I. A.; Kozhevnikov, V. L.; Mitberg, E. B.; Patrakeev, M. V.; Kharton, V. V.; Marques, F. M. B. *J. Mater. Chem.* **2001**, *11*, 1201.

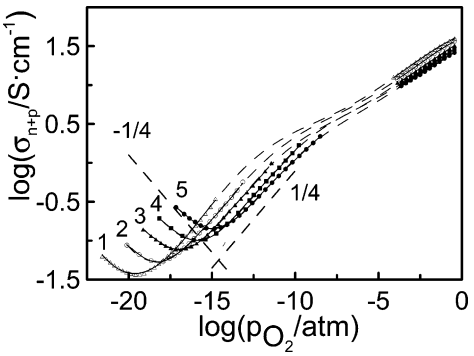

Figure 8. Logarithmic plots of the sum of the electron and hole contributions versus oxygen pressure for the solid solution $LaSr_2Fe_{3-y}Cr_yO_{8+\delta}$ at different temperatures: (1) 750, (2) 800, (3) 850, (4) 900, (5) 950 °C. The slopes of the isotherms left and right of the minima approach −1/4 and +1/4, respectively.

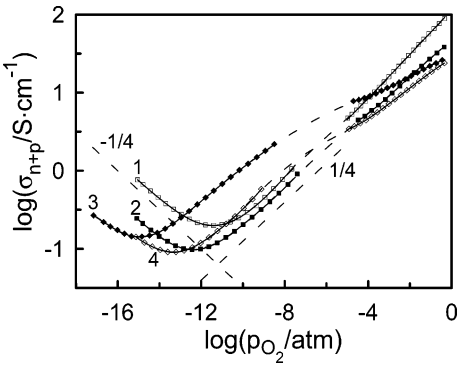

Figure 9. Pressure variations of electron−hole conductivity in $LaSr_2Fe_{3-y}Cr_yO_{8+\delta}$ at 950 °C: $y = 0$ (1), 0.3 (2), 0.6 (4), and 1.0 (3).

amount of oxygen (δ) in/from the structure of $LaSr_2Fe_{3-y}Cr_yO_{8+\delta}$ according to reactions $^1/_2O_2 = O^{2-} + 2h^+$ and $O^{2-} = {}^1/_2O_2 + 2e^-$, respectively. Because the oxygen content variations in the low-pressure region are small ($\delta \ll 1$) compared to the total amount of the oxygen in the crystal lattice, the oxygen concentration in the crystal lattice can be taken as invariable in the respective equilibrium constants, which results in the pressure dependencies for the partial contributions $\sigma_p \approx [h^+] \approx pO_2^{+1/4}$ and $\sigma_n \approx [e^-] \approx pO_2^{-1/4}$ consistent with the experiment.

The electron−hole conductivity isotherms versus oxygen partial pressure at 950 °C are shown for the samples with different doping in Figure 9. It can be noticed that larger isobaric values of the hole-type conductivity correspond to smaller values of the elementary unit parameter a_{rhomb} in Figure 4. This correlation is not unexpected because changes in a_{rhomb} reflect variations in the average length of chemical bonds (Fe,Cr)−O, i.e., in the bonding energy of the crystal lattice oxygen. Therefore, the oxygen loss is more ample and the amount of electron holes left in the lattice is smaller and, respectively, the conductivity level is smaller in specimens with larger a_{rhomb}. This trend is indeed seen in Figure 9 at $pO_2 \rightarrow 1$atm where σ_p for the sample with $y = 1$ (and relatively larger a_{rhomb}) is about four times smaller than for the sample with $y = 0$ (and relatively smaller a_{rhomb}), while in the oxygen depleted samples, which are stable at $pO_2 < 10^{-4}$ atm, the hole contribution to conductivity is about five times larger in the sample with $y = 1$ (and relatively smaller a_{rhomb}) than in the sample with $y = 0$ (and relatively larger a_{rhomb}). At pressures below about 10^{-12} atm, where dominating carriers are of n-type, the oxygen bonding energy increasing with chromium content results in oxygen loss smaller in samples with larger doping (at pO_2= const). Hence, both the amount of n-type carriers created in the crystal lattice in response to oxygen depletion and the level of conductivity tend to be smaller when chromium doping is larger.

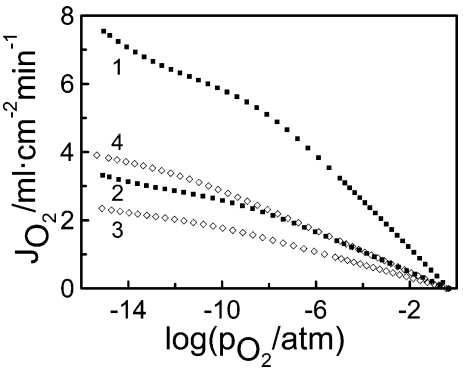

Figure 10. Estimated oxygen permeation flux through 0.1 cm thick membranes of the solid solution $LaSr_2Fe_{3-y}Cr_yO_{8+\delta}$ as a function of the permeate-side oxygen partial pressure at 950 °C. The feed-side oxygen partial pressure corresponds to atmospheric pressure. Numbers 1, 2, 3, and 4 correspond to the y values 0, 0.3, 0.6, and 1, respectively.

5. Oxygen Permeability and Thermal Expansion. The applicability of oxygen membrane materials depends essentially on their oxygen permeation fluxes. The dependence of the flux density jO_2 on the oxygen pressure difference across the membrane of thickness L can be calculated by using the measured total conductivity σ and calculated values σ_i for the ion conductivity according to known relation[20]

$$jO_2 = \frac{RT}{16F^2L}\int_{pO_2'}^{pO_2''}\frac{\sigma_i\cdot(\sigma - \sigma_i)}{\sigma}d\ln pO_2 \qquad (5)$$

where pO_2' and pO_2'' are the oxygen partial pressures at the membrane feed and permeate sides, respectively. These estimates give only an upper limit of oxygen permeation rate because surface exchange reactions may result in some suppression of the overall transport. For the conditions typical for syngas generation ($pO_2' = 0.21$ atm, $pO_2'' = 10^{-16}$ atm, 950 °C), the results for the membranes with $L = 0.1$ cm and different chromium contents are shown in Figure 10. In the calculations at high pressures the ion conductivity values were assumed to be nearly equal to those at low pressures, Table 2. As expected, the permeation rate in chromium doped samples is smaller than those in the parent ferrite. Nonetheless, it may achieve a value of about 4 $mL\cdot cm^{-2}\cdot min^{-1}$ in the sample with $y = 1$, which corresponds to the syngas production rate of about 20−25 $mL\cdot cm^{-2}\cdot min^{-1}$ in the methane partial oxidation process.

The relative linear thermal expansions in air and in high-purity helium ($pO_2 = 10^{-6}$ atm) for the ceramics with $y = 0$ and $y = 1$ are shown in Figure 11. Representative data for $Zr(Y)O_2$ in air are also given for comparison. At temperatures above 400 °C, where oxygen exchange with the environment develops, the dimensional changes increase rapidly with temperature

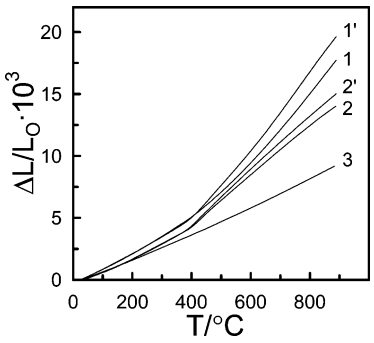

Figure 11. Relative linear expansion for oxide ceramics $LaSr_2Fe_{3-y}Cr_yO_{8+\delta}$ with $y = 0$ in air (1) and helium (1′) and $y = 1$ in air (2) and helium (2′). The data for $Zr(Y)O_2$ in air are shown for comparison (3).

in the ferrite with $y = 0$. The large difference of the expansion in helium and in air at a fixed temperature demonstrates that the major contribution to the change in linear dimensions observed in the parent ferrite at high temperatures is related to the loss of oxygen from the crystal lattice. It is interesting that this difference is appreciably smaller in the doped ferrite. In particular the chromium doped sample with $y = 1$ demonstrates better resistance toward dimensional deformations induced by the oxygen loss. Notice also that the combined temperature increase and oxygen depletion do not produce as large an expansion for the $y = 1$ sample compared to the parent ferrite, which seemingly is favored by the invariably rhombohedral structure of the oxide with $y = 1$.

Conclusions

Ceramic samples of chromium doped lanthanum−strontium ferrite $LaSr_2Fe_{3-y}Cr_yO_{8+\delta}$ ($y = 0$, 0.3, 0.6, and 1.0) were synthesized and characterized using X-ray diffraction, thermal gravimetry, dilatometry, and total conductivity measurements in the temperature range 750−950 °C at oxygen partial pressures varying between 10^{-22} and 0.5 atm. The air-synthesized samples have the rhombohedral $R\bar{3}c$ structure. The loss of oxygen from the crystal lattice results in formation of the oxygen vacancy ordered structure $LaSr_2Fe_3O_8$ for the parent ferrite at temperatures above 750 °C and oxygen pressures below about 10^{-5} atm while chromium doped samples $LaSr_2Fe_{3-y}Cr_yO_8$ ($y = 0.3$, 0.6, and 1.0) retain perovskite-like rhombohedral $R\bar{3}c$ structure. The experimental data for total conductivity were utilized to determine oxygen ion contribution in $LaSr_2Fe_{3-y}Cr_yO_8$ as a function of temperature and oxygen pressure. The isothermal ion conductivity was found to decrease with an increase with chromium doping from $y = 0$ to $y = 0.6$. Further increase in chromium content to $y = 1$ results in an increase of the ion conductivity. This behavior is shown to originate from partial involvement in the ion transport of oxygen ions coordinated by the chromium dopant in the ion transport mechanism. A permeation rate of about 4 $mL{\cdot}cm^{-2}{\cdot}min^{-1}$ of pure oxygen from air with a membrane of 0.1 cm thickness, which is equivalent to formation of about 20−25 $mL{\cdot}cm^{-2}{\cdot}min^{-1}$ of syngas in the methane partial oxidation process, was estimated for $y = 1$ using the conductivity data. In combination with good thermodynamic and structural stability, and moderate lattice thermal expansion, this permeation rate would indicate that the oxide $LaSr_2Fe_{3-y}Cr_yO_{8+\delta}$ is a promising candidate membrane material for the partial oxidation of natural gas.

Acknowledgment. This work was supported in part by the Russian Foundation for Basic Research under the grant 01-03-96519 and by the award 978002 of the NATO Science for Peace Program. K.R.P. is grateful to the EMSI program of the National Science Foundation and the U.S. Department of Energy, Office of Science (CHE-9810378) at the Northwestern University Institute for Environmental Catalysis.

CM031084O